*Psychoradiology*, 2025, **5**, kkaf001

DOI: 10.1093/psyrad/kkaf001
Advance access publication date: 7 February 2025
Research Article

# Abnormal arteriolar blood volume measured by 3D inflow-based vascular-space-occupancy (iVASO) MRI and resting-state BOLD fluctuations at 7 T in individuals with recent-onset schizophrenia

Andor L. Bodnár[1], Daniel A. Stevens[1], Adrian G. Paez[2,3], Kia Ultz[4], Christopher A. Ross[1,5,6], Jun Hua[2,3] and Russell L. Margolis[1,5,*]

[1]Schizoaffective Disorder Precision Medicine Center of Excellence, Division of Neurobiology, Department of Psychiatry and Behavioral Sciences, Johns Hopkins University School of Medicine, Baltimore, MD 21287, USA
[2]The Russell H. Morgan Department of Radiology and Radiological Science, Division of MR Research, Johns Hopkins University School of Medicine, Baltimore, MD 21287, USA
[3]F.M. Kirby Research Center for Functional Brain Imaging, Kennedy Krieger Institute, Baltimore, MD 21205, USA
[4]Institutional Review Board, University of Pennsylvania, Philadelphia, PA 19104, USA
[5]Department of Neurology, Johns Hopkins University School of Medicine, Baltimore, MD 21287, USA
[6]Departments of Neuroscience and Pharmacology, Johns Hopkins University School of Medicine, Baltimore, MD 21287, USA
*Correspondence: Russell L. Margolis, rmargoli@jhmi.edu

## Abstract

**Background:** We previously reported lower baseline arteriolar cerebral blood volumes (CBVa) in almost all gray matter regions in a cohort of individuals with schizophrenia of varying ages and disease duration. The extent to which decreased CBVa is also present in recent-onset schizophrenia, and how this impacts neurovascular coupling, remains to be determined. In this study, we sought to determine the extent of CBVa deficits in recent-onset schizophrenia and the relationship of CBVa to region-specific resting-state neural activity.

**Methods:** Using 7 T MRI, CBVa was measured in 90 regions using 3D inflow-based vascular-space-occupancy (iVASO) imaging in 16 individuals with recent-onset schizophrenia (disease duration: $\bar{x} = 1.18 \pm 1.4$ years) and 12 age-matched controls. Resting-state functional MRI (rs-fMRI) was used to determine fractional amplitudes of low-frequency fluctuations (fALFF) and intrinsic connectivity (ICC) in spontaneous blood oxygen level-dependent (BOLD) signal. The region-specific relationship between CBVa and fALFF was determined as an index of neurovascular coupling.

**Results:** Compared with healthy participants, CBVa was lower in individuals with schizophrenia in almost all brain regions, with a global effect size of 0.23 and regional effect sizes up to 0.41. Individuals with schizophrenia also exhibited lower fALFF diffusely across cortical and subcortical gray matter regions. Ratios of mean regional CBVa to fALFF and ICC were significantly lower in patients in numerous brain regions

**Conclusion:** These findings indicate that early-stage schizophrenia is characterized by widespread microvascular abnormalities and associated resting-state deficits in neural activity, suggesting that abnormalities in neurovascular coupling may contribute to the pathophysiology of schizophrenia.

## Introduction

Emerging evidence suggests that metabolic and microvascular abnormalities may be present in the early stages of schizophrenia and may contribute to disease pathogenesis (Meier *et al.*, 2013). The cerebral microvasculature is essential for meeting brain metabolic demands, as it regulates the delivery of oxygen and energy substrates to specific regions. (Harris *et al.*, 2013; Hua *et al.*, 2017). Cerebral microvascular function involves a variety of interconnected physiological processes, many of which may be disrupted in schizophrenia. These disruptions include widespread reductions in cerebral blood flow (CBF) (Zhu *et al.*, 2017; Selvaggi *et al.*, 2023) and impairments in the integrity of the blood–brain barrier (BBB) (Najjar *et al.*, 2017). Cerebral blood volume (CBV) is a an important and sensitive physiological parameter that measures the quantity of blood in a unit of tissue (ml blood/100 ml tissue) (Hua *et al.*, 2019). Baseline CBV indicates the stable state of the microvasculature in accordance with local brain metabolism, correlates with regional metabolic activity, and is sensitive to metabolic disturbances (Gonz *et al.*, 1995; Raichle, 1983). Previous studies suggest that baseline CBV is diffusely lower in individuals with schizophrenia, especially in the bilateral frontal and occipital cortices (Brambilla *et al.*, 2007; Peruzzo *et al.*, 2011), and may inversely correlate with disease duration (Bellani *et al.*, 2011). Additionally, alterations in CBV may serve as a predictor for the progression to psychosis in individuals at risk for developing schizophrenia (Schobel *et al.*, 2013; Schobel *et al.*, 2009).

Most research on CBV in schizophrenia has measured total CBV, which includes arterial, capillary, and venous signals. However, each type of blood vessel has unique metabolic functions that

**Received:** 7 November 2024; **Revised:** 31 December 2024; **Accepted:** 6 February 2025

may be differentially associated with schizophrenia pathophysiology, yet only about 25% of total CBV represents arterial blood volume (CBVa) (Hua, Liu, *et al.*, 2019; Piechnik *et al.*, 2008; Sharan *et al.*, 1989; van Zigl et al., 1998). Arterioles regulate cerebral perfusion through vasodilation and vasoconstriction, and are especially sensitive to metabolic disturbances (Iadecola & Nedergaard, 2007; Ito *et al.*, 2005; Ito *et al.*, 2001; Kim *et al.*, 2007). Animal models indicate that neurodegeneration first affects arterial vessels and later impacts capillaries and veins, suggesting that changes in arteriolar blood volume might be early indicators of metabolic dysfunction in schizophrenia (Balbi *et al.*, 2015). Therefore, measuring arteriolar changes may provide crucial information not readily accessible from total CBV (Hua *et al.*, 2019; Iadecola & Nedergaard, 2007; Ito *et al.*, 2005; Ito *et al.*, 2001; Takano et al., 2006).

CBVa can be assessed using inflow vascular-space-occupancy (iVASO) magnetic resonance imaging (MRI) (Donahue *et al.*, 2010; Hua, *et al.*, 2011), a noninvasive approach that does not require the administration of exogenous contrast agents. When coupled with ultrahigh field strength (7 T), it provides high signal-to-noise ratios (SNRs) (Hua, *et al.*, 2017, 2019; Wu et al., 2016). In general, the higher resolution of 7 T compared to 3 T improves SNR, with enhanced structural and temporal resolution (Calabro *et al.*, 2024). However, a few studies have implemented iVASO at 3 T (Gu *et al.*, 2024), including the measurement of arteriolar muscle blood volume in skeletal muscle of individuals with dermatomyositis (Liu *et al.*, 2021), the discrimination of histological grades of gliomas (Li *et al.*, 2019), the demonstration that hippocampal CBVa is greater than cortical CBVa in healthy volunteers (Rane *et al.*, 2016), and the absence of a detectable difference in hippocampal CBVa, measured in a single slice, between patients with early-stage psychosis and healthy volunteers (Talati *et al.*, 2016). Our group previously used iVASO to demonstrate lower CBVa in most cortical and subcortical regions in a heterogeneous group of schizophrenia patients, primarily with long disease duration, compared to matched controls. In the superior and middle temporal lobe, and in Heschel's gyri, CBVa was inversely proportional to disease duration (Hua *et al.*, 2017). Whether low CBVa reflects a fundamental disease pathophysiological process, a homeostatic response to a pathophysiological process, an epiphenomenon, or the effect of long-term treatment remains uncertain. CBV and CBF are also critical modulators of the blood-oxygen-level-dependent (BOLD) signal measured with functional MRI (fMRI) (Ogawa *et al.*, 1993; van Zijl et al., 1998).

In resting-state fMRI (rs-fMRI), spontaneous, regional low-frequency (0.01–0.1 Hz) BOLD fluctuations reflect the power of spontaneous neural activation and correlate with cognitive processes (Han *et al.*, 2011). Additionally, intrinsic connectivity (ICC), a measure of the global centrality of a voxel, helps define resting-state networks and identifies network hubs, regions where connectivity and basal metabolism are relatively high (Martuzzi *et al.*, 2011). Previous studies suggest a correlation between CBV/CBF and BOLD-derived measures, particularly the amplitude of low-frequency fluctuations (ALFF) and its fractional form (fALFF) (Deng *et al.*, 2022; Li *et al.*, 2012; Liang *et al.*, 2013). Regional ALFF, a temporally stable characteristic of spontaneous BOLD fluctuations in the 0.01–0.1 (Hz) frequency range, may reflect the intensity of local spontaneous neuronal activity (Fang *et al.*, 2021). Furthermore, regional neurovascular coupling of CBV/CBF and resting-state BOLD measures is disrupted in various diseases, including schizophrenia (Hu *et al.*, 2019; Sukumar *et al.*, 2020; Wang *et al.*, 2024; Wu *et al.*, 2024; Zhu *et al.*, 2017; Chen *et al.*, 2022). However, prior studies have not investigated the relationship between CBVa and BOLD fALFF or ICC. Our original finding was based on patients with a broad range of disease duration, and included five individuals with disease duration of <5 years, and only two with duration of <1 year (mean disease duration 19.0, SD 17.8 years), and did not explore the relationship between CBVa and BOLD-driven measurements (Hua *et al.*, 2017). Given the potential value of our previous CBVa finding, we sought to confirm this finding in a new population of recent-onset patients, and to extend the analysis to assess the relationship between CBVa and resting-state functional activity (fALFF and ICC) as an approach for investigating neurovascular decoupling.

To begin addressing these issues, we developed a pilot project to determine if CBVa is low very early in the course of schizophrenia, minimizing the confounding effects of age and disease duration, though recognizing that medicine remains an uncontrolled factor. In addition, we explored the relationship between CBVa and spontaneous BOLD fluctuations, focusing on ICC and fALFF, which has good temporal stability and is less susceptible to physiologic noise than ALFF (Küblböck *et al.*, 2014; *Zou* et al., 2008). We hypothesized that the ratio of CBVa to fALFF and ICC would be reduced early in schizophrenia, indicating that a part of the pathophysiology of schizophrenia may stem not only from deficits in CBVa levels, but also from an imbalance between arteriolar blood supply and neural activity reflecting disease-related disruptions of neurovascular coupling.

## Methods

### Participant recruitment and characterization

Sixteen participants with a recent diagnosis of schizophrenia were recruited from Johns Hopkins schizophrenia clinics, and 12 age-matched healthy controls were recruited from the community. Current schizophrenia symptom severity was assessed with the Positive and Negative Syndrome Scale for Schizophrenia (PANSS) (Kay *et al.*, 1987). None of the participants had other neurologic history or neurologic signs on exam, or a history of vascular diseases. All participants with schizophrenia were receiving antipsychotic medications at the time of study participation. All participants gave written informed consent. Recruitment and study protocols were approved by the Johns Hopkins Institutional Review Board (IRB) in concordance with the Declaration of Helsinki.

### MRI acquisition

Imaging was conducted with a 7 T Philips MRI scanner as previously described (see Hua *et al.*, 2017). Briefly, high-resolution anatomical scans were obtained through a 3D magnetization prepared 2 rapid acquisition gradient echoes (MP2RAGE) sequence with a voxel size of 0.65 mm isotropic. An rs-fMRI scan was performed with gradient echo (GRE) echo-planar imaging (EPI) (TR/TE/FA = 2000/22 ms/60°, voxel = 2.5 mm isotropic, 54 slices, 7 min) for each participant. For the measurement of gray matter (GM) CBVa, a 3D iVASO MRI technique with whole brain coverage was utilized (Hua *et al.*, 2017). Arterial blood signal was nullified through spatially selective inversion, and CBVa was derived from the difference between the nullified scan and a control scan. Interleaved images at various delay times account for vascular transit time heterogeneity, while crushing gradients suppress signals from large arteries. The iVASO technique, initially using GRE EPI for single-slice imaging, was extended to 3D whole-brain coverage with T1-enhanced TurboFLASH to minimize distortion and power deposition (Hua *et al.*, 2011, 2013; Donahue *et al.*,

2010). Specific iVASO parameters included TR/TI values ranging from 10 000/1383 to 2000/356 ms, a 3D fast GRE readout with TR-GRE/TEGRE of 4.2/2.2 ms, voxel dimensions of 3.5 × 3.5 × 5 mm over 20 slices, parallel imaging acceleration (SENSE) of 2 × 2, crusher gradients of $b = 0.3$ s/mm$^2$, and a velocity encoding (Venc) of 10 cm/s in the z-direction (Rooney et al., 2007). Additionally, a reference scan was obtained with a TR of 20 s and identical parameters to determine the scaling factor M0 for absolute CBVa value calculation.

## iVASO preprocessing

iVASO preprocessing was performed in native space using MATLAB 2017a. All iVASO images were motion-corrected with SPM12. Difference signals between arterial blood nulled and control iVASO images were calculated using the surround subtraction approach. Manual registration was conducted between iVASO and anatomical images due to differing image contrasts, with voxel size at 3.5 × 3.5 × 5 mm. Imaging volumes were matched and prescribed before scans, with any residual misalignment manually corrected (Gu *et al.*, 2024). For comparison with rs-fMRI, CBVa maps were warped to MNI-space, resampled to 2 mm isotropic voxels, and visually inspected for alignment with MNI-space structural and rs-fMRI scans.

## Resting-state fMRI preprocessing, denoising, and first-level analysis

Preprocessing, denoising, and first-level analysis of resting-state fMRI data were performed using CONN release 22.a (Whitfield-Gabrieli & Nieto-Castanon, 2012; Ashburner, 2016) and SPM release 12.7771 (Friston, 2007). Functional and anatomical data were preprocessed using a pipeline (Nieto-Castanon, 2020) that included realignment with susceptibility distortion correction, slice timing correction, outlier detection, indirect segmentation, MNI-space normalization, and smoothing. Functional data were realigned using SPM's realign & unwarp procedure (Andersson *et al.*, 2001) and corrected for temporal misalignment using SPM's slice-timing correction (Sladky *et al.*, 2011). Outliers were identified using ART obtained from www.nitrc.org (Whitfield-Gabrieli, 2011), and data were coregistered, normalized to MNI space, segmented, and resampled to 2 mm voxels (Calhoun *et al.*, 2017; Ashburner, 2007; Ashburner & Friston, 2005). Functional data were smoothed with an 8 mm FWHM Gaussian kernel.

Denoising included regression of confounding effects [white matter, cerebrospinal fluid (CSF), motion parameters, outliers, session and task effects, linear trends], followed by bandpass filtering of the BOLD timeseries between 0.01 and 0.1 Hz (Hallquist *et al.*, 2013). CompCor (Behzadi *et al.*, 2007; Chai *et al.*, 2012) noise components were estimated within white matter and CSF. Post-denoising degrees of freedom for the BOLD signal ranged from 41.4 to 112.3 across subjects. fALFF maps were calculated as the ratio of the root mean square (RMS) of the denoised BOLD signal within 0.01–0.1 Hz to the pre-filtered signal (Zou *et al.*, 2008). ICC maps were estimated from the RMS of all connections between each voxel and the rest of the brain, using singular value decomposition with 64 components for each subject (Martuzzi *et al.*, 2011; Whitfield-Gabrieli & Nieto-Castanon, 2012).

## Statistical analysis

In-house MATLAB code was used to extract mean regional CBVa measurements from voxel-wise CBVa maps generated during 3D iVASO preprocessing, using structural regions from the JHU Adult 286 labels 10 atlases V5L set. A 2 × 2 mixed-model ANOVA examined differences in regional CBVa values across brain regions (left vs. right hemisphere) and populations (healthy control vs. recent-onset schizophrenia). Student's t-tests analyzed between-group differences by region, with effect sizes estimated using partial eta squared ($\eta_p^2$). Regional CBVa values were compared with regional spontaneous BOLD signal fluctuations in MNI-space and mean regional CBVa values were extracted from MNI-transformed voxel-wise CBVa maps using the IBASPM 116 atlas. Voxel-wise beta maps from first-level fALFF and ICC analyses were used to extract mean regional beta values. One-way ANOVA assessed between-group differences in mean regional CBVa, fALFF, and ICC beta values. Neurovascular coupling was computed as the ratio of mean regional CBVa values to mean regional beta values from fALFF and ICC, with between-group differences assessed using Student's t-tests. Correlation of neurovascular coupling with symptom severity was evaluated using Pearson correlation between PANSS scores and mean regional CBVa/fALFF and CBVa/ICC values. Multiple linear regression, adjusted for age and sex, assessed regional correlation of CBVa, fALFF, and ICC with PANSS scores and disease duration, corrected for multiple comparisons using false-discovery rate (FDR) (adjusted $P < 0.05$). Voxel-wise between-group differences in CBVa, fALFF, and ICC were evaluated in MNI space using generalized linear models adjusted for age and sex, with significance thresholds of $P = 0.05$ unadjusted and $P = 0.05$ FDR-corrected for cluster size. Voxel-wise correlation of CBVa, fALFF, and ICC with PANSS scores was also assessed using general linear models adjusted for age and sex.

# Results

## Participant characteristics

For this pilot project, 16 participants with schizophrenia and 12 healthy control participants were recruited and completed study tasks and scans. Disease duration of individuals with schizophrenia was $\bar{x} = 1.18$ years (SD = 1.4). Age was closely matched (schizophrenia $\bar{x} = 23.4$ years, SD 3.3; controls $\bar{x} = 24.5$ years, SD 2.9). Sex ratios were: schizophrenia (male/female = 14/2) and controls (male/female = 7/5). Race of patients was: schizophrenia (White/Black = 11/5) and controls (White/Black = 6/6). PANSS scores of individuals with schizophrenia were 38–86 ($\bar{x} = 59.4$, SD = 14.2), indicating that the majority of the patients were mildly to moderately ill (Leucht *et al.*, 2005). One control participant was unable to complete the rs-fMRI scan. PANSS total scores were not significantly correlated with CBVa, fALFF, or ICC.

## Lower baseline CBVa in recent-onset schizophrenia

Global mean CBVa (cortex and subcortical GM) was lower in individuals with recently diagnosed schizophrenia compared with controls (Table 1, Fig. 1). Mean regional CBVa values were diffusely lower in multiple brain regions in individuals with schizophrenia compared to healthy controls with relative changes of 11.9–48.5% and effect sizes of 0.14–0.41. Lower CBVa was observed in both hemispheres in all cortical lobes and in most subcortical regions. In almost all brain regions where significant differences were not observed, CBVa levels were lower in schizophrenia patients. CBVa was greater in individuals with schizophrenia in the left cuneus and in the nucleus accumbens and basal forebrain, but these differences were not significant after correction for multiple comparisons (see Supplementary Table 1). In total,

**Table 1:** Lower baseline regional CBVa values in individuals with recently diagnosed schizophrenia.

| Region | Left hemisphere | | | Right hemisphere | | | Bilateral | | | | | |
|---|---|---|---|---|---|---|---|---|---|---|---|---|
| | Control | Schizophrenia | | Control | Schizophrenia | | Control | Schizophrenia | | | | |
| | Mean (SD) | Mean (SD) | Diff (%) | Mean (SD) | Mean (SD) | Diff (%) | Mean (SD) | Mean (SD) | Diff (%) | F | P | $\eta_p^2$ |
| **Global cortical** | **0.86 (0.12)** | **0.73 (0.12)** | **17.8** | **0.83 (0.10)** | **0.70 (0.10)** | **18.6** | **0.85 (0.11)** | **0.72 (0.11)** | **18.4** | **9.85** | **0.004 #** | **0.28** |
| **Frontal lobe** | **1.04 (0.16)** | **0.83 (0.2)** | **24.6** | **0.94 (0.14)** | **0.76 (0.17)** | **22.7** | **0.99 (0.15)** | **0.8 (0.19)** | **23.7** | **9.06** | **0.006 #** | **0.26** |
| **Parietal lobe** | **0.82 (0.15)** | **0.68 (0.08)** | **21.8** | **0.90 (0.15)** | **0.69 (0.09)** | **31.8** | **0.86 (0.15)** | **0.69 (0.1)** | **26.8** | **17.01** | **0.000 #** | **0.40** |
| **Temporal lobe** | **0.90 (0.27)** | **0.7 (0.16)** | **28.5** | **0.79 (0.18)** | **0.64 (0.08)** | **24.0** | **0.85 (0.23)** | **0.67 (0.12)** | **26.3** | **7.80** | **0.010** | **0.23** |
| **Occipital lobe** | **0.77 (0.09)** | **0.75 (0.1)** | **1.6** | **0.93 (0.13)** | **0.79 (0.12)** | **18.25*** | **0.85 (0.11)** | **0.77 (0.11)** | **9.9** | 3.79 | 0.062 | 0.13 |
| **Cingulate** | **0.82 (0.18)** | **0.69 (0.16)** | **18.6** | **0.82 (0.14)** | **0.71 (0.18)** | **16.0** | **0.82 (0.16)** | **0.7 (0.17)** | **17.3** | 3.82 | 0.062 | 0.13 |
| **Parahippocampal gyrus** | 0.83 (0.25) | 0.73 (0.18) | 12.0 | 0.78 (0.19) | 0.69 (0.15) | 11.5 | 0.81 (0.22) | 0.72 (0.17) | 12.5 | 2.06 | 0.160 | 0.07 |
| **Entorhinal cortex** | 0.85 (0.32) | 0.82 (0.40) | 4.2 | 0.75 (0.2) | 0.70 (0.17) | 7.6 | 0.80 (0.26) | 0.76 (0.29) | 5.9 | 0.25 | 0.619 | 0.01 |
| **Hippocampus** | 0.73 (0.12) | 0.66 (0.12) | 9.6 | 0.71 (0.13) | 0.62 (0.07) | 12.7 | 0.72 (0.13) | 0.65 (0.10) | 10.8 | 3.88 | 0.060 | 0.13 |
| **Amygdala** | 0.82 (0.18) | 0.68 (0.08) | 20.5 | 0.74 (0.19) | 0.66 (0.12) | 9.9 | 0.78 (0.19) | 0.67 (0.10) | 15.2 | **4.29** | **0.048** | **0.14** |
| **Nucleus accumbens** | 0.72 (0.09) | 0.76 (0.27) | -5.6 | 0.69 (0.08) | 0.71 (0.19) | -2.9 | 0.71 (0.09) | 0.74 (0.23) | -4.1 | 0.14 | 0.71 | 0.01 |
| **Basal forebrain** | 0.75 (0.15) | 0.72 (0.25) | 4.0 | 0.73 (0.13) | 0.65 (0.07) | 11.0 | 0.74 (0.14) | 0.72 (0.22) | 3.4 | 1.26 | 0.270 | 0.05 |
| **Thalamus** | **0.75 (0.10)** | **0.65 (0.06)** | **15.8** | **0.70 (0.08)** | **0.64 (0.06)** | **8.0** | **0.73 (0.09)** | **0.65 (0.06)** | **11.9** | **9.68** | **0.004 #** | **0.27** |
| **Basal ganglia** | **0.68 (0.09)** | **0.65 (0.10)** | **4.4** | **0.65 (0.06)** | **0.62 (0.05)** | **4.6** | **0.67 (0.07)** | **0.63 (0.08)** | **6.0** | 1.457 | 0.238 | 0.05 |
| **Brain stem** | **0.77 (0.12)** | **0.66 (0.10)** | **14.3** | **0.75 (0.08)** | **0.68 (0.09)** | **9.3** | **0.76 (0.10)** | **0.67 (0.10)** | **11.8** | **5.78** | **0.024** | **0.18** |
| **Cerebellum** | **0.93 (0.28)** | **0.69 (0.09)** | **34.9** | **0.89 (0.34)** | **0.65 (0.10)** | **37.7** | **0.91 (0.31)** | **0.67 (0.10)** | **36.3** | **9.34** | **0.005 #** | **0.26** |

Regional mean baseline arteriolar cerebral blood volume CBVa (ml/100 ml) for healthy control participants and participants recently diagnosed with schizophrenia. Two-way ANOVA was used to assess differences between groups. Effect size was calculated using partial eta squared ($\eta_p^2$). Bold and italicized entries indicate significantly reduced regional mean CBVa ($P < 0.05$) in individuals with schizophrenia, while # = differences exceeding a false discovery rate (FDR) corrected P-value of 0.05. * = post-hoc t-test results showing significant differences in unilateral regional CBVa between participants with schizophrenia and controls at an uncorrected P-value of <0.05.

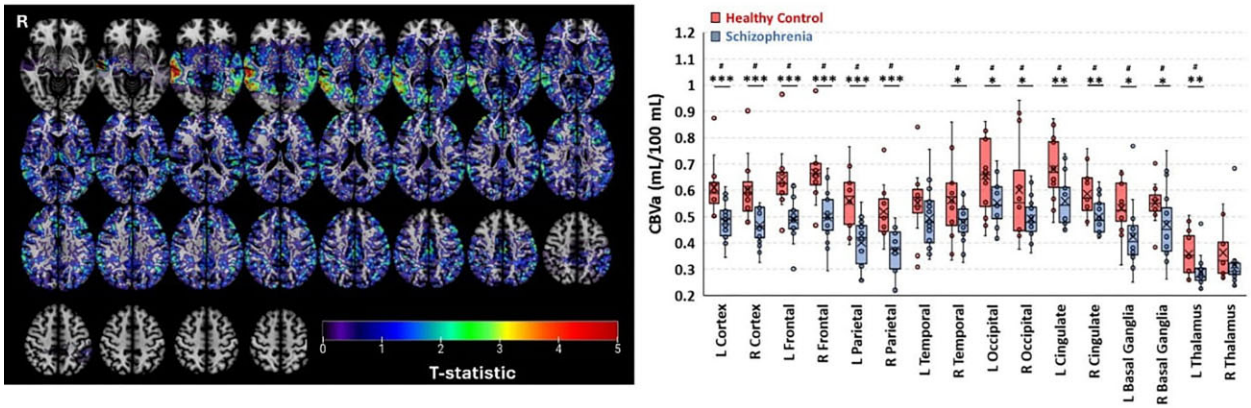


**Figure 1:** Mean regional CBVa is lower in individuals with recently diagnosed schizophrenia.
(**Left**) Depiction of voxel-wise differences in gray matter CBVa between individuals recently diagnosed with schizophrenia and healthy controls, adjusted for age and sex, and superimposed on an MNI-space standard template. (**Right**) Boxplot depicting the group mean and distribution of CBVa levels (in ml/100 ml tissue) for select regions in healthy control participants (red) and individuals recently diagnosed with schizophrenia (blue). Student's t-tests were used to compare the group means. Statistical significance is depicted as follows: $*P < 0.05$, $**P < 0.01$, $***P < 0.001$ uncorrected; # indicates significant differences exceeding an FDR-corrected $P < 0.05$. CBVa = arteriolar cerebral blood volume.

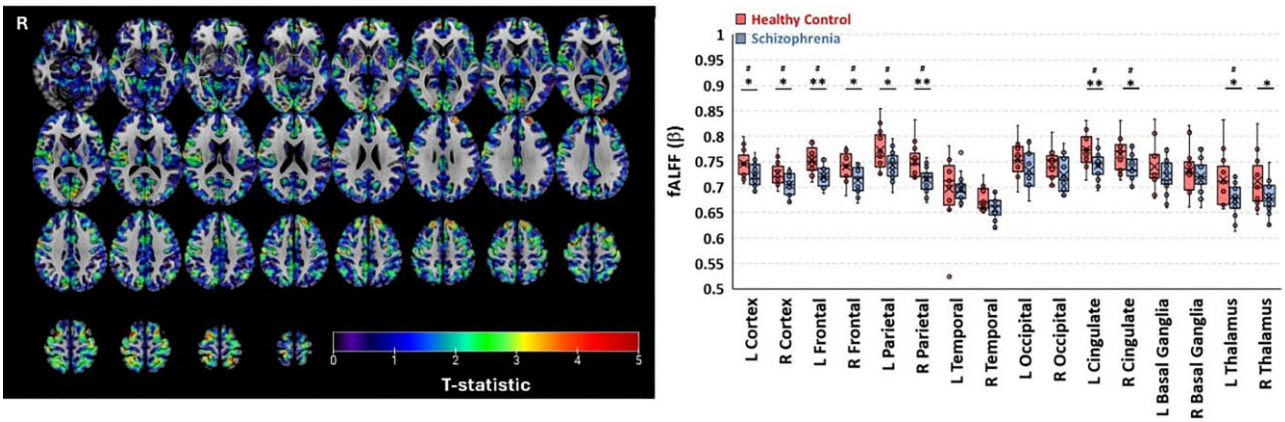


**Figure 2:** Individuals with recently diagnosed schizophrenia show lower fractional amplitudes of low-frequency, spontaneous BOLD fluctuations.
(**Left**) Depiction of voxel-wise differences in fALFF between individuals recently diagnosed with schizophrenia and healthy controls, adjusted for age and sex, and superimposed on an MNI-space standard template. (**Right**) Boxplot depicting the group mean and distribution of fALFF for select regions in healthy control participants (red) and individuals recently diagnosed with schizophrenia (blue). Student's t-tests were used to compare the group means. Statistical significance is depicted as follows: $*P < 0.05$, $**P < 0.01$, $***P < 0.001$. # indicates significant differences exceeding an FDR-corrected $P < 0.05$. fALFF = fractional amplitude of low-frequency fluctuations, BOLD = blood oxygen level dependent.

15/24 frontal subregions had significantly reduced CBVa in individuals with schizophrenia (ranging from 9.2 to 44.5%; $\eta_p^2 = 0.16$–$0.39$). CBVa was decreased in individuals with schizophrenia in 10/10 parietal subregions (13.0–41.4% change; $\eta_p^2 = 0.29$–$0.40$) and in 12/12 temporal subregions (16.3–48.5% change; $\eta_p^2 = 0.17$–$0.29$). CBVa in the insular cortices and cerebellum were also significantly reduced in individuals with schizophrenia (10.8–37.7% change; $\eta_p^2 = 0.15$–$0.26$) along with 5/10 occipital regions (16.4–32.1% change; $\eta_p^2 = 0.25$–$0.26$). CBVa was reduced in both anterior and posterior cingulate cortices in individuals with schizophrenia (6/10 regions; 11.3–19.5% change; $\eta_p^2 = 0.21$–$0.41$). Mean regional CBVa values did not correlate with PANSS scores.

Gray matter CBVa was also examined using voxel-wise differences in standard MNI space (Fig. 1, Supplementary Table 2). Consistent with the native space results, CBVa was significantly lower in schizophrenia patients in the bilateral frontal, parietal, occipital, and cingulate cortices, and in the left temporal cortex and in the left thalamus after adjustment for age and sex, and after FDR correction for multiple comparisons.

## Reduced CBVa ratios and fALFF values in recent-onset schizophrenia

Individuals with schizophrenia exhibited lower fALFF than control participants in multiple cortical and thalamic regions (Fig. 2). Regional between-group differences in fALFF reached statistical significance in the frontal, parietal, and right occipital lobes as well as in the cingulate cortices and thalamus. fALFF values were also decreased, though not to the level of statistical significance, in the temporal and occipital cortices, and in the basal ganglia.

Subregional analysis of between-group differences in fALFF were conducted for cortical and subcortical regions defined by the IBASPM atlas. fALFF values were slightly and nonsignificantly

**Table 2:** Recently diagnosed schizophrenia is associated with lower regional CBVa per unit of fALFF.

| Region | Left hemisphere | | | | | | | | Right hemisphere | | | | | | | |
|---|---|---|---|---|---|---|---|---|---|---|---|---|---|---|---|---|
| | Control | | Schizophrenia | | | | | | Control | | Schizophrenia | | | | | |
| | Mean | SE | Mean | SE | Diff (%) | T | P | P-FDR | Mean | SE | Mean | SE | % | T | P | P-FDR |
| Precentral | 0.71 | 0.07 | 0.53 | 0.04 | 29 | 2.24 | 0.017 | 0.062 | **0.70** | **0.06** | **0.52** | **0.04** | **30** | **2.54** | **0.009** | **0.047** |
| Frontal_Sup | 0.75 | 0.08 | 0.65 | 0.05 | 14 | 1.11 | 0.139 | 0.212 | 0.86 | 0.08 | 0.64 | 0.06 | 29 | 2.18 | 0.019 | 0.064 |
| Frontal_Sup_Orb | 1.20 | 0.18 | 0.87 | 0.14 | 32 | 1.88 | 0.036 | 0.079 | 1.15 | 0.16 | 0.87 | 0.13 | 28 | 1.83 | 0.040 | 0.085 |
| Frontal_Mid | 0.86 | 0.09 | 0.68 | 0.04 | 23 | 2.11 | 0.023 | 0.069 | **1.02** | **0.08** | **0.76** | **0.05** | **29** | **2.94** | **0.004** | **0.030** |
| Frontal_Mid_Orb *(lateral)* | 0.89 | 0.15 | 0.64 | 0.07 | 33 | 2.09 | 0.023 | 0.069 | 0.95 | 0.14 | 0.63 | 0.09 | 41 | 2.19 | 0.019 | 0.064 |
| Frontal_Inf_Oper | 0.67 | 0.05 | 0.60 | 0.02 | 11 | 1.40 | 0.088 | 0.148 | 0.83 | 0.06 | 0.76 | 0.07 | 9 | 0.76 | 0.226 | 0.294 |
| Frontal_Inf_Tri | 0.68 | 0.05 | 0.58 | 0.02 | 16 | 2.11 | 0.023 | 0.069 | 0.78 | 0.06 | 0.70 | 0.06 | 11 | 0.92 | 0.184 | 0.258 |
| Frontal_Inf_Orb | 0.67 | 0.09 | 0.55 | 0.07 | 20 | 1.00 | 0.164 | 0.235 | 0.75 | 0.10 | 0.66 | 0.06 | 13 | 1.06 | 0.151 | 0.222 |
| Rolandic_Oper | 0.74 | 0.06 | 0.65 | 0.03 | 13 | 1.39 | 0.089 | 0.148 | 0.79 | 0.07 | 0.73 | 0.06 | 8 | 0.63 | 0.267 | 0.334 |
| Supp_Motor_Area | 0.69 | 0.08 | 0.49 | 0.06 | 34 | 1.96 | 0.031 | 0.072 | 0.63 | 0.07 | 0.48 | 0.07 | 27 | 1.53 | 0.069 | 0.126 |
| Olfactory | 1.95 | 0.32 | 1.38 | 0.23 | 34 | 1.48 | 0.075 | 0.133 | 1.79 | 0.28 | 1.26 | 0.17 | 35 | 1.72 | 0.049 | 0.101 |
| Frontal_Sup_Medial | 0.83 | 0.06 | 0.76 | 0.06 | 9 | 0.82 | 0.210 | 0.286 | 0.88 | 0.06 | 0.80 | 0.06 | 10 | 0.80 | 0.217 | 0.291 |
| Frontal_Mid_Orb *(medial)* | **2.30** | **0.31** | **1.14** | **0.20** | **67** | **3.67** | **0.001** | **0.013** | **1.94** | **0.26** | **0.96** | **0.15** | **68** | **3.67** | **0.001** | **0.013** |
| Rectus | 1.63 | 0.31 | 1.38 | 0.29 | 17 | 0.31 | 0.379 | 0.443 | 1.60 | 0.32 | 1.24 | 0.27 | 25 | 0.35 | 0.364 | 0.437 |
| Insula | 0.81 | 0.04 | 0.73 | 0.03 | 10 | 1.57 | 0.065 | 0.122 | 1.00 | 0.09 | 0.81 | 0.05 | 21 | 2.01 | 0.028 | 0.071 |
| Cingulum_Ant | 1.14 | 0.11 | 0.95 | 0.08 | 18 | 1.35 | 0.094 | 0.151 | 0.92 | 0.08 | 0.79 | 0.05 | 15 | 1.58 | 0.063 | 0.121 |
| Cingulum_Mid | **0.75** | **0.03** | **0.67** | **0.02** | **11** | **2.67** | **0.007** | **0.037** | 0.71 | 0.03 | 0.65 | 0.02 | 9 | 1.97 | 0.030 | 0.072 |
| Cingulum_Post | 0.53 | 0.02 | 0.50 | 0.02 | 6 | 0.87 | 0.197 | 0.273 | 0.43 | 0.03 | 0.43 | 0.02 | 0 | −0.01 | 0.502 | 0.565 |
| Hippocampus | 0.68 | 0.07 | 0.70 | 0.06 | −3 | −0.28 | 0.609 | 0.660 | 0.63 | 0.07 | 0.67 | 0.05 | −6 | −0.52 | 0.696 | 0.739 |
| Parahippocampal | 0.45 | 0.08 | 0.56 | 0.07 | −22 | −1.08 | 0.854 | 0.884 | 0.47 | 0.07 | 0.64 | 0.07 | −31 | −1.70 | 0.949 | 0.949 |
| Amygdala | 0.72 | 0.10 | 0.68 | 0.09 | 6 | −0.17 | 0.568 | 0.624 | 0.74 | 0.06 | 0.75 | 0.07 | −1 | −0.74 | 0.768 | 0.804 |
| Calcarine | 0.94 | 0.05 | 0.80 | 0.05 | 16 | 1.94 | 0.032 | 0.073 | 0.63 | 0.04 | 0.57 | 0.02 | 10 | 1.49 | 0.075 | 0.133 |
| Cuneus | 0.90 | 0.06 | 0.87 | 0.06 | 3 | 0.32 | 0.374 | 0.443 | 0.73 | 0.05 | 0.73 | 0.04 | 0 | 0.05 | 0.479 | 0.545 |
| Lingual | **0.96** | **0.07** | **0.74** | **0.03** | **26** | **3.31** | **0.001** | **0.018** | **1.07** | **0.12** | **0.70** | **0.03** | **42** | **3.37** | **0.001** | **0.018** |
| Occipital_Sup | 0.87 | 0.06 | 0.74 | 0.05 | 16 | 1.74 | 0.048 | 0.099 | 0.73 | 0.06 | 0.68 | 0.05 | 7 | 0.67 | 0.255 | 0.323 |
| Occipital_Mid | 0.89 | 0.07 | 0.73 | 0.04 | 20 | 2.04 | 0.026 | 0.069 | 0.76 | 0.05 | 0.68 | 0.04 | 11 | 1.27 | 0.109 | 0.171 |
| Occipital_Inf | **1.32** | **0.21** | **0.76** | **0.07** | **54** | **2.91** | **0.004** | **0.030** | **1.25** | **0.21** | **0.73** | **0.06** | **53** | **2.72** | **0.006** | **0.037** |
| Fusiform | 0.64 | 0.09 | 0.69 | 0.04 | −8 | −0.52 | 0.698 | 0.739 | 0.78 | 0.13 | 0.70 | 0.04 | 11 | 0.61 | 0.274 | 0.338 |
| Postcentral | 0.64 | 0.05 | 0.51 | 0.03 | 23 | 2.24 | 0.017 | 0.062 | **0.61** | **0.05** | **0.45** | **0.03** | **30** | **2.69** | **0.006** | **0.037** |
| Parietal_Sup | **0.81** | **0.10** | **0.48** | **0.06** | **51** | **3.20** | **0.002** | **0.021** | **0.79** | **0.11** | **0.37** | **0.06** | **72** | **3.70** | **0.001** | **0.013** |
| Parietal_Inf | 0.89 | 0.06 | 0.71 | 0.04 | 23 | 2.40 | 0.012 | 0.055 | 0.90 | 0.07 | 0.69 | 0.05 | 26 | 2.40 | 0.012 | 0.055 |
| Supra_Marginal | 0.76 | 0.07 | 0.63 | 0.02 | 19 | 2.25 | 0.017 | 0.062 | **0.76** | **0.05** | **0.63** | **0.03** | **19** | **2.48** | **0.010** | **0.050** |
| Angular | 0.95 | 0.07 | 0.76 | 0.05 | 22 | 2.34 | 0.014 | 0.060 | 0.83 | 0.05 | 0.71 | 0.05 | 16 | 1.65 | 0.056 | 0.111 |
| Precuneus | **0.69** | **0.04** | **0.49** | **0.03** | **34** | **4.23** | **0.000** | **0.009** | **0.63** | **0.04** | **0.52** | **0.02** | **19** | **2.73** | **0.006** | **0.037** |
| Paracentral_Lobule | 0.36 | 0.05 | 0.23 | 0.04 | 44 | 2.25 | 0.017 | 0.062 | 0.35 | 0.03 | 0.25 | 0.04 | 33 | 2.04 | 0.026 | 0.069 |
| Caudate | 0.90 | 0.07 | 0.73 | 0.05 | 21 | 2.06 | 0.025 | 0.069 | 0.84 | 0.06 | 0.72 | 0.06 | 15 | 1.35 | 0.094 | 0.151 |
| Putamen | 0.74 | 0.05 | 0.59 | 0.05 | 23 | 1.93 | 0.033 | 0.073 | 0.81 | 0.05 | 0.69 | 0.06 | 16 | 1.47 | 0.077 | 0.134 |
| Pallidum | 0.18 | 0.04 | 0.13 | 0.02 | 32 | 1.04 | 0.155 | 0.225 | 0.32 | 0.05 | 0.28 | 0.04 | 13 | 0.59 | 0.280 | 0.340 |
| Thalamus | 0.50 | 0.04 | 0.43 | 0.02 | 15 | 1.61 | 0.060 | 0.118 | 0.50 | 0.04 | 0.47 | 0.04 | 6 | 0.67 | 0.254 | 0.323 |
| Heschl | 0.79 | 0.05 | 0.69 | 0.02 | 14 | 1.98 | 0.030 | 0.072 | 0.87 | 0.08 | 0.76 | 0.05 | 13 | 1.24 | 0.114 | 0.177 |
| Temporal_Sup | **0.91** | **0.07** | **0.73** | **0.03** | **22** | **2.83** | **0.005** | **0.034** | **1.02** | **0.09** | **0.75** | **0.05** | **31** | **3.45** | **0.001** | **0.016** |
| Temporal_Pole_Sup | 0.42 | 0.07 | 0.41 | 0.06 | 2 | 1.07 | 0.148 | 0.221 | 0.64 | 0.10 | 0.59 | 0.06 | 8 | 0.78 | 0.222 | 0.294 |
| Temporal_Mid | 1.09 | 0.11 | 0.85 | 0.06 | 25 | 2.04 | 0.026 | 0.069 | **1.15** | **0.11** | **0.82** | **0.04** | **34** | **3.15** | **0.002** | **0.021** |
| Temporal_Pole_Mid | 0.19 | 0.17 | 0.41 | 0.09 | −73 | −1.36 | 0.907 | 0.928 | 0.16 | 0.06 | 0.29 | 0.08 | −58 | −1.70 | 0.949 | 0.949 |
| Temporal_Inf | 0.77 | 0.14 | 0.79 | 0.09 | −3 | −0.13 | 0.551 | 0.612 | 0.84 | 0.12 | 0.81 | 0.06 | 4 | 0.28 | 0.390 | 0.450 |

Regional mean values for the ratio of arteriolar cerebral blood volume CBVa (ml/100 ml) to fractional amplitudes of low-frequency BOLD fluctuations for healthy control participants ($n = 11$) and participants recently diagnosed with schizophrenia ($n = 16$). Student's t-tests were used to compare the regional mean values between groups and P-FDR values were adjusted for the number of regions tested (90 regions) using the Benjamini–Hochberg method for false discovery rate (FDR) correction. Bold and italicized entries indicate significantly lower regional mean CBVa/fALFF in the schizophrenia group at an FDR-adjusted P-value of 0.05.

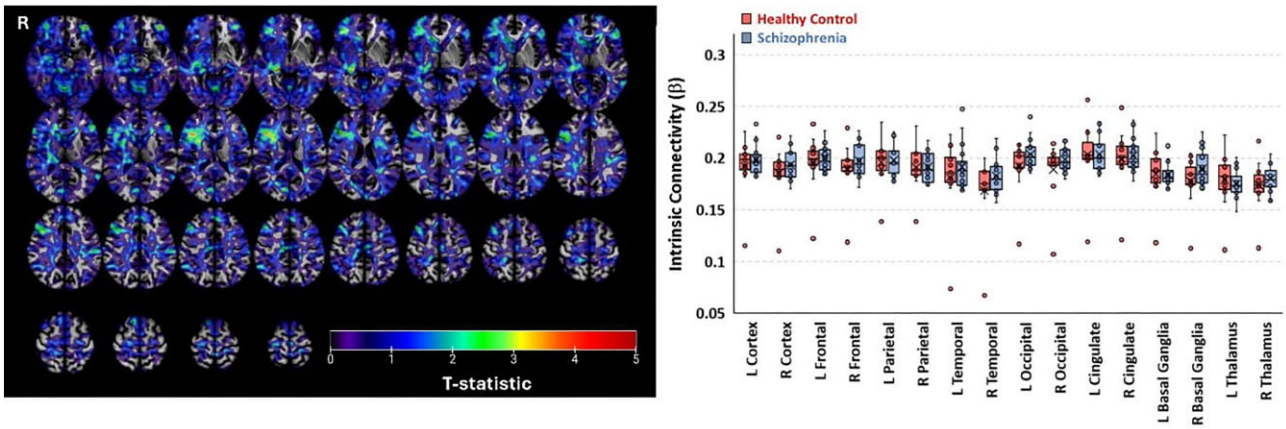


**Figure 3:** Regional mean intrinsic connectivity does not differ between controls and individuals with recently diagnosed schizophrenia.(**Left**) Depiction of voxel-wise comparisons of ICC between individuals recently diagnosed with schizophrenia and healthy controls, adjusted for age and sex, and superimposed on an MNI-space standard template. **(Right)** Boxplot depicting the group mean and distribution of regional average intrinsic connectivity values for select regions in healthy control participants (red) and individuals recently diagnosed with schizophrenia (blue). Student's t-tests were used to compare the group means, none were significant.

decreased in most regions in individuals with schizophrenia. Equal values were noted in the right and left inferior orbital frontal cortex, left hippocampus, and left mid-temporal pole. Values were slightly but not significantly increased in the right and left parahippocampus, right and left fusiform cortex, right and left superior temporal pole, right and left inferior temporal cortex, right superior orbital cortex, right rectal gyrus, right hippocampus, and right amygdala (Supplementary Table 3).

CBVa per unit of fALFF was calculated across 90 cortical and subcortical regions (Table 2). After FDR correction, the ratio was significantly lower in individuals with schizophrenia in 18 specific regions: the right precentral gyrus, right middle frontal gyrus, left and right medial orbital frontal cortices, left mid-cingulate cortex, right middle and bilateral superior temporal cortices, bilateral precuneus, left supramarginal gyrus, bilateral superior parietal regions, as well as the left postcentral gyrus, bilateral lingual gyri, and bilateral inferior occipital gyri. There were also nonsignificant increases in CBVa/fALFF ratio in individuals with schizophrenia in bilateral parahippocampal gyri and hippocampus, left amygdala, left fusiform gyrus, left inferior temporal gyrus, and bilateral mid-temporal poles.

There were no statistically significant differences between groups in ICC (Fig. 3, Supplementary Table 4). The ratio of CBVa to ICC was significantly lower in individuals with schizophrenia in 51 brain regions, and nonsignificantly decreased in an additional nine regions. Higher but nonsignificant CBVa to ICC ratios were found in the right parahippocampal gyrus and in bilateral mid-temporal poles (Table 3).

## Discussion

This pilot study using 7 T MRI revealed diffusely lower CBVa in both cortical and subcortical gray matter regions in individuals with a recent diagnosis of schizophrenia compared to age-matched healthy controls. This finding aligns with our previous work, which examined a more heterogeneous schizophrenia population that included relatively few recent-onset cases (Hua *et al.*, 2017), along with observations of a number of previous studies that detected lower total CBV and CBF in schizophrenia patients (Schobel *et al.*, 2009; Peruzzo *et al.*, 2011; Malaspina *et al.*, 2004; Schulz *et al.*, 2002; Weinberger *et al.*, 1986; Zhu *et al.*, 2015; Faget-Agius *et al.*, 2012; Eisenberg *et al.*, 2010; Andreasen *et al.*, 1997; Ota *et al.*, 2014; Pinkham *et al.*, 2011; Walther *et al.*, 2011; Kanahara *et al.*, 2013; Kindler *et al.*, 2015; Tsujino *et al.*, 2011). A few studies have reported greater total CBV in schizophrenia in some brain regions, including parts of the occipital cortex, cerebellum, orbitofrontal cortex, hippocampus and basal ganglia (Loeber *et al.*, 1999; Cohen *et al.*, 1995; Malaspina *et al.*, 2004; Andreasen *et al.*, 1997; Tsujino *et al.*, 2011; Eisenberg *et al.*, 2010). The signal from decreased CBVa may have been insufficient to affect the total CBV result, though patient characteristics, including disease duration, may also have contributed to the different findings. Our previous study identified only small clusters of voxels with elevated CBVa in schizophrenia (Hua *et al.*, 2017). A previous test of a hypothesized increase in patient hippocampal CBVa using iVASO at 3 T in a single slice found no difference between early psychosis patients and controls (Talati *et al.*, 2016), not inconsistent with our current finding of an nonsignificant decrease in hippocampal CBVa. In the current study, CBVa was increased only in the left cuneus and in the nucleus accumbens and basal forebrain, but these differences were not significant after correction for multiple comparisons. It is possible that increased total CBV detected in other studies reflects increased volume in vascular compartments other than the arterioles. Our results, specific to the arteriolar compartment, suggest that widespread microvascular abnormalities are typically present no later than 1 year after schizophrenia diagnosis.

Next, using rs-fMRI at 7 T we observed that individuals recently diagnosed with schizophrenia exhibited lower fALFF values globally, with the most robust differences in the frontal lobes. ICC was also diffusely lower, but this did not reach statistical significance. Previous work suggests that schizophrenia is associated with differences in the amplitudes of spontaneous BOLD fluctuations. While the regions implicated and the direction of effect have been inconsistent, abnormal fALFF values have been described in first-episode drug-naive schizophrenia patients compared to healthy controls in the right inferior temporal gyrus (Fang *et al.*, 2021). Our results extend these findings by demonstrating decreased fALFF in multiple brain regions and in the setting of antipsychotic medicines.

We detected lower CBVa/fALFF and CBVa/ICC ratios across wide areas of the brain in recent-onset schizophrenia. A reduced CBVa/fALFF ratio suggests diminished arteriolar blood

**Table 3:** Recently diagnosed schizophrenia is associated with lower regional CBVa per unit of intrinsic connectivity.

| Region | Left hemisphere | | | | | | | | Right hemisphere | | | | | | | |
|---|---|---|---|---|---|---|---|---|---|---|---|---|---|---|---|---|
| | Control | | Schizophrenia | | | | | | Control | | Schizophrenia | | | | | |
| | Mean | SE | Mean | SE | Diff (%) | T | P | P-FDR | Mean | SE | Mean | SE | % | T | P | P-FDR |
| Precentral | **2.89** | **0.28** | **2.01** | **0.16** | **36** | **2.96** | **0.003** | **0.017** | **2.88** | **0.23** | **1.96** | **0.17** | **38** | **3.26** | **0.002** | **0.012** |
| Frontal_Sup | 2.94 | 0.31 | 2.37 | 0.20 | 21 | 1.63 | 0.058 | 0.082 | **3.42** | **0.35** | **2.39** | **0.22** | **35** | **2.64** | **0.007** | **0.023** |
| Frontal_Sup_Orb | **4.95** | **0.83** | **3.22** | **0.54** | **42** | **2.24** | **0.017** | **0.036** | **4.86** | **0.72** | **3.21** | **0.51** | **41** | **2.36** | **0.013** | **0.032** |
| Frontal_Mid | **3.26** | **0.30** | **2.46** | **0.14** | **28** | **2.71** | **0.006** | **0.021** | **3.99** | **0.28** | **2.76** | **0.19** | **36** | **3.75** | **0.001** | **0.009** |
| Frontal_Mid_Orb *(lateral)* | **3.66** | **0.61** | **2.35** | **0.27** | **44** | **2.57** | **0.008** | **0.024** | **3.96** | **0.61** | **2.32** | **0.33** | **52** | **2.76** | **0.005** | **0.020** |
| Frontal_Inf_Oper | **2.62** | **0.23** | **2.13** | **0.09** | **21** | **2.26** | **0.017** | **0.036** | **3.25** | **0.25** | **2.58** | **0.20** | **23** | **2.07** | **0.025** | **0.044** |
| Frontal_Inf_Tri | **2.61** | **0.16** | **2.08** | **0.09** | **23** | **3.17** | **0.002** | **0.013** | **3.13** | **0.24** | **2.47** | **0.19** | **24** | **2.15** | **0.021** | **0.040** |
| Frontal_Inf_Orb | 2.76 | 0.46 | 1.96 | 0.26 | 34 | 1.64 | 0.057 | 0.081 | 3.20 | 0.49 | 2.40 | 0.22 | 29 | 1.87 | 0.036 | 0.059 |
| Rolandic_Oper | **2.88** | **0.27** | **2.26** | **0.11** | **24** | **2.35** | **0.013** | **0.032** | 3.02 | 0.25 | 2.49 | 0.19 | 19 | 1.69 | 0.052 | 0.077 |
| Supp_Motor_Area | **2.81** | **0.31** | **1.84** | **0.24** | **42** | **2.53** | **0.009** | **0.025** | 2.56 | 0.30 | 1.78 | 0.26 | 36 | 1.94 | 0.032 | 0.053 |
| Olfactory | 9.32 | 2.54 | 5.15 | 0.92 | 58 | 1.77 | 0.045 | 0.070 | **8.38** | **1.81** | **4.64** | **0.63** | **57** | **2.23** | **0.018** | **0.036** |
| Frontal_Sup_Medial | 3.26 | 0.33 | 2.71 | 0.23 | 18 | 1.43 | 0.083 | 0.108 | 3.48 | 0.32 | 2.98 | 0.25 | 15 | 1.24 | 0.113 | 0.143 |
| Frontal_Mid_Orb *(medial)* | **9.05** | **1.37** | **4.03** | **0.68** | **77** | **3.95** | **0.000** | **0.009** | **7.66** | **1.15** | **3.39** | **0.52** | **77** | **3.92** | **0.000** | **0.009** |
| Rectus | 7.00 | 1.66 | 5.00 | 1.08 | 33 | 0.75 | 0.231 | 0.250 | 7.42 | 2.18 | 4.53 | 1.00 | 48 | 0.90 | 0.188 | 0.219 |
| Insula | 3.06 | 0.35 | 2.52 | 0.12 | 19 | 1.71 | 0.050 | 0.075 | **3.88** | **0.53** | **2.71** | **0.16** | **36** | **2.47** | **0.010** | **0.026** |
| Cingulum_Ant | 4.36 | 0.55 | 3.43 | 0.30 | 24 | 1.61 | 0.060 | 0.083 | 3.62 | 0.47 | 2.87 | 0.20 | 23 | 1.66 | 0.055 | 0.080 |
| Cingulum_Mid | 3.09 | 0.35 | 2.49 | 0.06 | 22 | 2.03 | 0.027 | 0.047 | 2.92 | 0.34 | 2.40 | 0.07 | 20 | 1.81 | 0.041 | 0.065 |
| Cingulum_Post | 2.18 | 0.13 | 1.91 | 0.09 | 13 | 1.73 | 0.048 | 0.073 | 1.76 | 0.17 | 1.62 | 0.09 | 8 | 0.76 | 0.229 | 0.250 |
| Hippocampus | 2.81 | 0.30 | 2.53 | 0.21 | 10 | 0.79 | 0.220 | 0.247 | 2.66 | 0.32 | 2.39 | 0.17 | 11 | 0.81 | 0.213 | 0.242 |
| ParaHippocampal | 2.17 | 0.71 | 2.04 | 0.24 | 6 | 0.20 | 0.420 | 0.435 | 2.14 | 0.50 | 2.27 | 0.23 | −6 | −0.26 | 0.603 | 0.617 |
| Amygdala | 3.26 | 0.80 | 2.45 | 0.32 | 28 | 0.69 | 0.249 | 0.264 | 3.81 | 1.13 | 2.63 | 0.25 | 37 | 0.72 | 0.240 | 0.257 |
| Calcarine | **3.80** | **0.26** | **2.93** | **0.17** | **26** | **2.92** | **0.004** | **0.017** | **2.57** | **0.20** | **2.07** | **0.10** | **22** | **2.44** | **0.011** | **0.027** |
| Cuneus | 3.59 | 0.26 | 3.21 | 0.18 | 11 | 1.27 | 0.108 | 0.139 | 2.97 | 0.21 | 2.70 | 0.15 | 10 | 1.06 | 0.149 | 0.183 |
| Lingual | **3.97** | **0.42** | **2.63** | **0.14** | **41** | **3.50** | **0.001** | **0.010** | **4.40** | **0.58** | **2.54** | **0.14** | **54** | **3.68** | **0.001** | **0.009** |
| Occipital_Sup | **3.45** | **0.24** | **2.76** | **0.19** | **22** | **2.24** | **0.017** | **0.036** | 2.87 | 0.23 | 2.58 | 0.19 | 11 | 1.01 | 0.160 | 0.195 |
| Occipital_Mid | **3.49** | **0.25** | **2.65** | **0.17** | **27** | **2.93** | **0.004** | **0.017** | 2.98 | 0.19 | 2.49 | 0.16 | 18 | 1.94 | 0.032 | 0.053 |
| Occipital_Inf | **5.12** | **0.78** | **2.69** | **0.27** | **62** | **3.35** | **0.001** | **0.012** | **5.09** | **0.85** | **2.69** | **0.24** | **62** | **3.16** | **0.002** | **0.013** |
| Fusiform | 2.98 | 0.76 | 2.44 | 0.15 | 20 | 0.83 | 0.207 | 0.238 | 3.39 | 0.61 | 2.56 | 0.17 | 28 | 1.53 | 0.069 | 0.093 |
| Postcentral | **2.64** | **0.20** | **1.94** | **0.13** | **31** | **3.07** | **0.003** | **0.013** | **2.48** | **0.21** | **1.71** | **0.14** | **37** | **3.22** | **0.002** | **0.012** |
| Parietal_Sup | **3.22** | **0.38** | **1.85** | **0.22** | **54** | **3.32** | **0.001** | **0.012** | **3.19** | **0.45** | **1.46** | **0.24** | **74** | **3.68** | **0.001** | **0.009** |
| Parietal_Inf | **3.46** | **0.27** | **2.63** | **0.16** | **27** | **2.77** | **0.005** | **0.020** | **3.54** | **0.23** | **2.53** | **0.21** | **33** | **3.11** | **0.002** | **0.013** |
| SupraMarginal | **2.99** | **0.30** | **2.30** | **0.08** | **26** | **2.59** | **0.008** | **0.024** | **2.91** | **0.23** | **2.29** | **0.09** | **24** | **2.88** | **0.004** | **0.017** |
| Angular | **3.61** | **0.29** | **2.71** | **0.20** | **28** | **2.66** | **0.007** | **0.022** | 3.17 | 0.22 | 2.60 | 0.19 | 20 | 1.93 | 0.033 | 0.053 |
| Precuneus | **2.75** | **0.19** | **1.91** | **0.10** | **36** | **4.11** | **0.000** | **0.009** | **2.49** | **0.16** | **1.98** | **0.10** | **23** | **2.86** | **0.004** | **0.017** |
| Paracentralobule | **1.50** | **0.20** | **0.92** | **0.15** | **48** | **2.59** | **0.008** | **0.024** | **1.49** | **0.17** | **0.97** | **0.15** | **42** | **2.30** | **0.015** | **0.034** |
| Caudate | **3.81** | **0.31** | **2.84** | **0.20** | **29** | **2.70** | **0.006** | **0.021** | **3.69** | **0.30** | **2.88** | **0.21** | **25** | **2.31** | **0.015** | **0.034** |
| Putamen | **2.91** | **0.19** | **2.33** | **0.19** | **22** | **2.08** | **0.024** | **0.044** | **3.23** | **0.21** | **2.51** | **0.19** | **25** | **2.48** | **0.010** | **0.026** |
| Pallidum | 0.74 | 0.18 | 0.53 | 0.09 | 33 | 1.15 | 0.130 | 0.163 | 1.26 | 0.18 | 1.09 | 0.15 | 14 | 0.75 | 0.231 | 0.250 |
| Thalamus | **2.01** | **0.16** | **1.65** | **0.09** | **20** | **2.09** | **0.024** | **0.044** | 2.11 | 0.20 | 1.75 | 0.13 | 19 | 1.58 | 0.063 | 0.086 |
| Heschl | **3.22** | **0.42** | **2.43** | **0.09** | **28** | **2.18** | **0.019** | **0.039** | 3.60 | 0.53 | 2.65 | 0.17 | 30 | 1.97 | 0.030 | 0.052 |
| Temporal_Sup | **3.55** | **0.41** | **2.64** | **0.12** | **29** | **2.48** | **0.010** | **0.026** | **4.12** | **0.48** | **2.70** | **0.19** | **42** | **3.25** | **0.002** | **0.012** |
| Temporal_Pole_Sup | 1.76 | 0.34 | 1.46 | 0.23 | 19 | 0.98 | 0.168 | 0.201 | 2.73 | 0.61 | 2.12 | 0.22 | 25 | 1.49 | 0.076 | 0.100 |
| Temporal_Mid | **4.39** | **0.66** | **3.10** | **0.23** | **34** | **2.12** | **0.022** | **0.043** | **4.67** | **0.54** | **2.98** | **0.16** | **44** | **3.52** | **0.001** | **0.010** |
| Temporal_Pole_Mid | 0.67 | 0.62 | 1.54 | 0.28 | −79 | −1.44 | 0.918 | 0.929 | 0.61 | 0.20 | 1.07 | 0.29 | −55 | −1.71 | 0.950 | 0.950 |
| Temporal_Inf | 3.61 | 1.09 | 2.94 | 0.37 | 20 | 0.67 | 0.256 | 0.267 | 3.53 | 0.52 | 3.03 | 0.25 | 15 | 0.96 | 0.172 | 0.204 |

Regional mean values for the ratio of arteriolar cerebral blood volume CBVa (ml/100 ml) to BOLD intrinsic connectivity for healthy control participants ($n = 11$) and participants recently diagnosed with schizophrenia ($n = 16$). Student's t-tests were used to compare the regional mean values between groups and P-values were adjusted for the number of regions tested (90 regions) using the Benjamini–Hochberg method for false discovery rate (FDR) correction. Bold and italicized entries indicate significantly lower regional mean CBVa/ICC in the schizophrenia group at an FDR-adjusted P-value of 0.05

supply relative to neural demands of cortical and subcortical regions (neurovascular uncoupling). Similarly, the widespread reduced CBVa/ICC ratio suggests that multiple brain regions, defined by their internal connectivity, receive a diminished supply of arteriolar blood. These results are consistent with previous studies examining relationships between total CBV/CBF to BOLD signal characteristics and metabolic measures in healthy individuals (Deng *et al.*, 2022; Li *et al.*, 2012; Liang *et al.*, 2013), and in schizophrenia (Zhu *et al.*, 2017; Sukumar *et al.*, 2020; Chen *et al.*, 2022). Decreased CBF relative to connectivity measures has been detected in cortical and subcortical regions in first-episode schizophrenia, along with an increase of this ratio in the sensorimotor cortex (Zhu *et al.*, 2017). These findings, like the findings reported in the present study, are consistent with evidence of neurovascular decoupling early in the course of schizophrenia, with differences in the direction of the decoupling in specific regions potentially related to the greater symptom severity and longer disease duration of participants in previous studies, and the distinctions between CBF and CBVa. Similar evidence of neurovascular coupling abnormalities has been detected in brain tumors, diabetes, kidney disease, mitochondrial encephalomyopathy with lactic acidosis and stroke-like episodes (MELAS), Parkinson's disease, and bipolar disorder (Abidin *et al.*, 2018; Agarwal *et al.*, 2016; Hu *et al.*, 2019; Wang *et al.*, 2024; Wu *et al.*, 2024). Neurovascular decoupling in schizophrenia may derive from multiple interrelated pathophysiological mechanisms: intrinsic impairment of the microvasculature (e.g. impaired nitric oxide release by vascular endothelial cells) (Kraal *et al.*, 2019), potentially related to metabolic inadequacy (Eelen *et al.*, 2018); dysregulation of astrocytic-mediated neurovascular signal transmission (Kameyama *et al.*, 2023; Bernstein *et al.*, 2025 ); abnormalities of the BBB (Kealy *et al.*, 2020; Puvogel *et al.*, 2022; Stanca *et al.*, 2024); inflammatory processes (Rossetti *et al.*, 2024; Kempuraj *et al.* 2024); and imbalance of excitatory and inhibitory neural transmission (Han *et al.*, 2020). Which, if any, of these processes will prove amenable to therapeutic intervention remains to be determined.

While exploratory, our observations are consistent with a hypothesis of impaired arteriolar dysregulation and neurovascular coupling present no later than ~1 year after the initial diagnosis of schizophrenia (Hanson & Gottesman, 2005; Sukumar *et al.*, 2020). Widespread microvascular abnormalities and neurovascular uncoupling may indicate insufficient support for synaptic activity, which over time could contribute to inflammation, mitochondrial dysfunction and oxidative stress, ultimately increasing neuronal dysfunction (Stanimirovic & Friedman, 2012; Watts *et al.*, 2018; Yan *et al.*, 2022). The individuals with recent-onset schizophrenia in this study were both medicated and had relatively well-controlled symptoms, suggesting that neither medicines nor symptom amelioration fully correspond to neurovascular coupling.

The size and scope of this study have potential implications for its generalizability. First, the sample size is modest. Nonetheless, effect sizes distinguishing patients from controls are quite robust, and the results are consistent with our earlier exploration of CBVa in schizophrenia that included individuals at all stages of disease duration (Hua *et al.*, 2017). Second, the limited clinical data and the cross-sectional study design are insufficient to determine whether decreased CBVa is a direct consequence of the pathophysiological processes of schizophrenia or a result of secondary factors, such as comorbidities or pharmacological treatment. Moreover, it remains unclear whether microvascular abnormalities and neurovascular decoupling play a direct role in functional disruption leading to the schizophrenia clinical phenotype, represent an epiphenomenon, or serve as a compensatory response to ongoing pathogenesis. Larger scale longitudinal studies, potentially including manipulations of the vascular system, will be necessary to address these issues, and to determine if CBVa and neurovascular decoupling correlate with clinical features of schizophrenia, such as treatment resistance or prominent negative symptoms.

## Supplementary data

Supplementary data are available at *PSYRAD Journal* online.

## Author contributions

Andor L. Bodnár (Formal analysis, Visualization, Writing – original draft, Writing – review & editing, Software), Daniel A. Stevens (Formal analysis, Visualization, Writing – original draft, Writing – review & editing, Software), Adrian G. Paez (Data curation, Data collection), Kia Ultz (Data curation, Investigation, Project administration), Christopher A. Ross (Supervision, Writing – review & editing), Jun Hua (Conceptualization, Funding acquisition, Investigation, Methodology, Resources, Software, Supervision, Writing – review & editing), and Russell L. Margolis (Conceptualization, Funding acquisition, Investigation, Resources, Supervision, Writing – original draft, Writing - review & editing)

## Conflict of interest

None.

## Acknowledgements

The authors thank the study participants for their willingness to support this investigation, and the faculty and staff of the Kirby Center for valuable advice and support. . This work was funded by NIMH T32MH015330, NIMH R21MH107016, NIBIB P41EB031771, the Abramson Fund, and the ABCD Charitable Trust.

## References

Abidin AZ, D'Souza AM, Nagarajan MB, *et al.* (2018) Alteration of brain network topology in HIV-associated neurocognitive disorder: A novel functional connectivity perspective. *Neuroimage Clin* **17**:768–77.

Agarwal S., Sair HI, Airan R, *et al.* (2016) Demonstration of brain tumor-induced neurovascular uncoupling in resting-state fMRI at ultrahigh field. *Brain Connect* **6**:267–72.

Andersson JL, Hutton C, Ashburner J, *et al.* (2001) Modeling geometric deformations in EPI time series. *NeuroImage* **13**:903–19.

Andreasen NC, O'Leary DS, Flaum M, *et al.* (1997) Hypofrontality in schizophrenia: distributed dysfunctional circuits in neuroleptic-naïve patients. *Lancet* **349**:1730–4.

Ashburner J. (2007) A fast diffeomorphic image registration algorithm. *NeuroImage* **38**:95–113.

Ashburner J. (2016) Preparing fMRI data for statistical analysis. In M. Filippi (ed). *fMRI Techniques and Protocols, Neuomethods, vol 119*. New York, NY: Humana Press, 155–81.

Ashburner J, Friston KJ (2005) Unified segmentation. *NeuroImage* **26**:839–51.

Balbi M, Ghosh M, Longden TA, *et al.* (2015) Dysfunction of mouse cerebral arteries during early aging. *J Cereb Blood Flow Metab* **35**:1445–53.

Bellani M, Peruzzo D, Isola M, *et al.* (2011) Cerebellar and lobar blood flow in schizophrenia: a perfusion weighted imaging study. *Psychiatr Res* **193**:46–52.

Bernstein HG, Nussbaumer M, Vasilevska V, *et al.* (2025) Glial cell deficits are a key feature of schizophrenia: implications for neuronal circuit maintenance and histological differentiation from classical neurodegeneration. *Molec Psychiatr* **30**:1102–16.

Brambilla P, Cerini R, Fabene PF, *et al.* (2007) Assessment of cerebral blood volume in schizophrenia: a magnetic resonance imaging study. *J Psychiatr Res* **41**:502–10.

Calabro FJ, Parr AC, Sydnor VJ, *et al.* (2024) Leveraging ultra-high field 7T MRI in psychiatric research. *Neuropsychopharmacol* **50**:85–102.

Calhoun VD, Wager TD, Krishnan A, *et al.* (2017) The impact of T1 versus EPI spatial normalization templates for fMRI data analyses. *Hum Brain Mapp* **38**:5331–42.

Chen J, Xue K, Yang M, *et al.* (2022) Altered coupling of cerebral blood flow and functional connectivity strength in first-episode schizophrenia patients with auditory verbal hallucinations. *Front Neurosci* **16**:821078.

Cohen BM, Yurgelun-Todd D, English CD, *et al.* (1995) Abnormalities of regional distribution of cerebral vasculature in schizophrenia detected by dynamic susceptibility contrast MRI. *Am J Psychiatry* **152**:1801–3.

Deng S, Franklin CG, O'Boyle M, *et al.* (2022) Hemodynamic and metabolic correspondence of resting-state voxel-based physiological metrics in healthy adults. *Neuroimage* **250**:118923.

Donahue MJ, Sideso E, MacIntosh BJ, *et al.* (2010) Absolute arterial cerebral blood volume quantification using inflow vascular-space-occupancy with dynamic subtraction magnetic resonance imaging. *J Cereb Blood Flow Metab* **30**:1329–42.

Eelen G, de Zeeuw P, Treps L, *et al.* (2018) Endothelial cell metabolism. *Physiol Rev* **98**:3–58.

Eisenberg DP, Berman KF (2010) Executive function, neural circuitry, and genetic mechanisms in schizophrenia. *Neuropsychopharmacol* **35**:258–77.

Faget-Agius C, Boyer L, Padovani R, *et al.* (2012) Schizophrenia with preserved insight is associated with increased perfusion of the precuneus. *J Psychiatr Neurosci* **37**:297–304.

Fang X, Zhang R, Bao C, *et al.* (2021) Abnormal regional homogeneity (ReHo) and fractional amplitude of low-frequency fluctuations (fALFF) in first-episode drug-naïve schizophrenia patients comorbid with depression. *Brain Imaging Behav* **15**:2627–36.

Gonz RG, Fischman AJ, Guimaraes AR, *et al.* (1995) Functional MR in the evaluation of dementia: correlation of abnormal dynamic cerebral blood volume measurements with changes in cerebral metabolism on positron emission tomography with fludeoxyglucose F 18. *Am J Neuroradiol* **16**:1763–70.

Gu C, Li Y, Cao D, *et al.* (2024) On the optimization of 3D inflow-based vascular-space-occupancy (iVASO) MRI for the quantification of arterial cerebral blood volume (CBVa). *Magn Reson Med* **91**:1893–907.

Hallquist MN, Hwang K, Luna B (2013) The nuisance of nuisance regression: spectral misspecification in a common approach to resting-state fMRI preprocessing reintroduces noise and obscures functional connectivity. *Neuroimage* **82**:208–25.

Han S, Becker B, Duan X, *et al.* (2020) Distinct striatum pathways connected to salience network predict symptoms improvement and resilient functioning in schizophrenia following risperidone monotherapy. *Schizophr Res* **215**:89–96.

Han Y, Wang J, Zhao Z, *et al.* (2011) Frequency-dependent changes in the amplitude of low-frequency fluctuations in amnestic mild cognitive impairment: a resting-state fMRI study. *Neuroimage* **55**:287–95.

Hanson DR, Gottesman II (2005) Theories of schizophrenia: a genetic-inflammatory-vascular synthesis. *BMC Med Genet* **6**:7.

Harris LW, Guest PC, Wayland MT, *et al.* (2013) Schizophrenia: metabolic aspects of aetiology, diagnosis and future treatment strategies. *Psychoneuroendocrin* **38**:752–66.

Hu B, Yan LF, Sun Q, *et al.* (2019) Disturbed neurovascular coupling in type 2 diabetes mellitus patients: evidence from a comprehensive fMRI analysis. *Neuroimage Clin* **22**:101802.

Hua J, Brandt AS, Lee S, *et al.* (2017) Abnormal grey matter arteriolar cerebral blood volume in schizophrenia measured with 3D inflow-based vascular-space-occupancy MRI at 7T. *Schizophr Bull* **43**:620–32.

Hua J, Lee S, Blair NI, *et al.* (2019) Increased cerebral blood volume in small arterial vessels is a correlate of amyloid-$\beta$–related cognitive decline. *Neurobiol Aging* **76**:181–93.

Hua J, Liu P, Kim T, *et al.* (2019) MRI techniques to measure arterial and venous cerebral blood volume. *Neuroimage* **187**:17–31.

Hua J, Qin Q, Donahue MJ, *et al.* (2011) Inflow-based vascular-space-occupancy (iVASO) MRI. *Magn Reson Med* **66**:40–56.

Iadecola C, Nedergaard M (2007) Glial regulation of the cerebral microvasculature. *Nat Neurosci* **10**:1369–76.

Ito H, Ibaraki M, Kanno I, *et al.* (2005) Changes in the arterial fraction of human cerebral blood volume during hypercapnia and hypocapnia measured by positron emission tomography. *J Cereb Blood Flow Metab* **25**:852–7.

Ito H, Kanno I, Iida H, *et al.* (2001) Arterial fraction of cerebral blood volume in humans measured by positron emission tomography. *Ann Nucl Med* **15**:111–6.

Kameyama T, Miyata M, Shiotani H, *et al.* (2023) Heterogeneity of perivascular astrocyte endfeet depending on vascular regions in the mouse brain. *iScience* **26**:108010.

Kanahara N, Sekine Y, Haraguchi T, *et al.* (2013) Orbitofrontal cortex abnormality and deficit schizophrenia. *Schizophr Res* **143**:246–52.

Kay SR, Fiszbein A, Opler LA (1987) The positive and negative syndrome scale (PANSS) for schizophrenia. *Schizophr Bull* **13**:261–76.

Kealy J, Greene C, Campbell M (2020) Blood-brain barrier regulation in psychiatric disorders. *Neurosci Lett* **726**:133664.

Kempuraj D, Dourvetakis KD, Cohen J, *et al.* (2024) Neurovascular unit, neuroinflammation and neurodegeneration markers in brain disorders. *Front Cell Neurosci* **18**:1491952.

Kim T, Hendrich KS, Masamoto K, *et al.* (2007) Arterial versus total blood volume changes during neural activity-induced cerebral blood flow change: implication for BOLD fMRI. *J Cereb Blood Flow Metab* **27**:1235–47.

Kindler J, Jann K, Homan P, *et al.* (2015) Static and dynamic characteristics of cerebral blood flow during the resting state in schizophrenia. *Schizophr Bull* **41**:163–70.

Kraal AZ, Moll AC, Arvanitis NR, *et al.* (2019) Metabolic syndrome is negatively associated with cognition among endothelial nitric oxide synthase (eNOS)- 786C carriers in schizophrenia-spectrum disorders. *J Psychiatr Res* **117**:142–7

Kühlböck M, Woletz M, Höflich A, *et al.* (2014) Stability of low-frequency fluctuation amplitudes in prolonged resting-state fMRI. *Neuroimage* **103**:249–57.

Li X, Liao S, Hua J, *et al.* (2019) Association of glioma grading with inflow-based vascular-space-occupancy MRI: a preliminary study at 3T. *J Magn Reson Imaging* **50**:1817–23.

Li Z, Zhu Y, Childress AR, *et al.* (2012) Relations between BOLD fMRI-derived resting brain activity and cerebral blood flow. *PLoS One* **7**:e44556.

Liang X, Zou Q, He Y, *et al.* (2013) Coupling of functional connectivity and regional cerebral blood flow reveals a physiological basis for network hubs of the human brain. *Proc Natl Acad Sci U S A* **110**:1929–34.

Liu X, Li X, Guo L, *et al.* (2021) Decreased muscular perfusion in dermatomyositis: initial results detected by inflow-based vascular-space-occupancy MRI. *Am J Roentgenol* **216**:1588–95.

Loeber RT, Sherwood AR, Renshaw PF, *et al.* (1999) Differences in cerebellar blood volume in schizophrenia and bipolar disorder. *Schizophr Res* **37**:81–9.

Malaspina D, Harkavy-Friedman J, Corcoran C, *et al.* (2004) Resting neural activity distinguishes subgroups of schizophrenia patients. *Biol Psychiatry* **56**:931–7.

Martuzzi R, Ramani R, Qiu M, *et al.* (2011) A whole-brain voxel based measure of intrinsic connectivity contrast reveals local changes in tissue connectivity with anesthetic without a priori assumptions on thresholds or regions of interest. *Neuroimage* **58**:1044–50.

Meier MH, Shalev I, Moffitt TE, *et al.* (2013) Microvascular abnormality in schizophrenia as shown by retinal imaging. *Am J Psychiatry* **170**:1451–9.

Najjar S, Pahlajani S, De Sanctis V, *et al.* (2017) Neurovascular unit dysfunction and blood-brain barrier hyperpermeability contribute to schizophrenia neurobiology: a theoretical integration of clinical and experimental evidence. *Front Psychiatry* **8**:83.

Ogawa S, Menon RS, Tank DW, *et al.* (1993) Functional brain mapping by blood oxygenation level-dependent contrast magnetic resonance imaging. A comparison of signal characteristics with a biophysical model. *Biophys J* **64**:803–12.

Ota M, Sato N, Sakai K, *et al.* (2014) Altered coupling of regional cerebral blood flow and brain temperature in schizophrenia compared with bipolar disorder and healthy subjects. *J Cereb Blood Flow Metabol* **34**:1868–72.

Peruzzo D, Rambaldelli G, Bertoldo A, *et al.* (2011) The impact of schizophrenia on frontal perfusion parameters: a DSC-MRI study. *J Neural Transm* **118**:563–70.

Piechnik SK, Chiarelli PA, Jezzard P (2008) Modelling vascular reactivity to investigate the basis of the relationship between cerebral blood volume and flow under CO2 manipulation. *Neuroimage* **39**:107–18.

Pinkham A, Loughead J, Ruparel K, *et al.* (2011) Resting quantitative cerebral blood flow in schizophrenia measured by pulsed arterial spin labeling perfusion MRI. *Psychiatry Res Neuroimaging* **194**:64–72.

Puvogel S, Palma V, Sommer IEC. (2022) Brain vasculature disturbance in schizophrenia. *Curr Opin Psychiatry* **35**:146–56.

Raichle ME (1983) Positron emission tomography. *Annu Rev Neurosci* **6**:249–67.

Rane S, Talati P, Donahue MJ, *et al.* (2016) Inflow-vascular space occupancy (iVASO) reproducibility in the hippocampus and cortex at different blood water nulling times. *Magn Reson Med* **75**:2379–87.

Rossetti M, Stanca S, Panichi LB, *et al.* (2024) Brain metabolic profiling of schizophrenia: a path towards a better understanding of the neuropathogenesis of psychosis. *Metab Brain Dis* **40**:28.

Schobel SA, Chaudhury NH, Khan UA, *et al.* (2013) Imaging patients with psychosis and a mouse model establishes a spreading pattern of hippocampal dysfunction and implicates glutamate as a driver. *Neuron* **78**:81–93.

Schobel SA, Lewandowski NM, Corcoran CM, *et al.* (2009) Differential targeting of the CA1 subfield of the hippocampal formation by schizophrenia and related psychotic disorders. *Arch Gen Psychiatry* **66**:938–46.

Schultz SK, O'Leary DS, Boles Ponto LL, *et al.* (2002) Age and regional cerebral blood flow in schizophrenia: age effects in anterior cingulate, frontal, and parietal cortex. *J Neuropsychiatry Clin Neurosci* **14**:19–24.

Selvaggi P, Jauhar S, Kotoula V, *et al.* (2023) Reduced cortical cerebral blood flow in antipsychotic-free first-episode psychosis and relationship to treatment response. *Psychol Med* **53**:5235–45.

Sharan M, Jones MD, Koehler RC, *et al.* (1989) A compartmental model for oxygen transport in brain microcirculation. *Ann Biomed Eng* **17**:13–38.

Sladky R, Friston KJ, Tröstl J, *et al.* (2011) Slice-timing effects and their correction in functional MRI. *Neuroimage* **58**:588–94.

Stanca S, Rossetti M, Bokulic Panichi L, *et al.* (2024) The cellular dysfunction of the brain-blood barrier from endothelial cells to astrocytes: the pathway towards neurotransmitter impairment in schizophrenia *Int J Mol Sci* **25**:1250.

Stanimirovic DB, Friedman A (2012) Pathophysiology of the neurovascular unit: disease cause or consequence?. *J Cereb Blood Flow Metab* **32**:1207–21.

Sukumar N, Sabesan P, Anazodo U, *et al.* (2020) Neurovascular uncoupling in schizophrenia: a bimodal meta-analysis of brain perfusion and glucose metabolism. *Front Psychiatry* **11**:754.

Takano T, Tian GF, Peng W, *et al.* (2006) Astrocyte-mediated control of cerebral blood flow. *Nat Neurosci* **9**:260–7.

Talati P, Rane S, Donahue MJ, *et al.* (2016) Hippocampal arterial cerebral blood volume in early psychosis. *Psychiatry Res Neuroimaging* **256**:21–5.

Tsujino N, Nemoto T, Yamaguchi T, *et al.* (2011) Cerebral blood flow changes in very-late-onset schizophrenia-like psychosis with catatonia before and after successful treatment. *Psychiatry Clin Neurosciences* **65**:600–3.

van Zijl PC, Eleff SM, Ulatowski JA, *et al.* (1998) Quantitative assessment of blood flow, blood volume and blood oxygenation effects in functional magnetic resonance imaging. *Nat Med* **4**:159–67.

Walther S, Federspiel A, Horn H, *et al.* (2011) Resting state cerebral blood flow and objective motor activity reveal basal ganglia dysfunction in schizophrenia. *Psychiatry Res* **192**:117–24.

Wang R, Liu X, Sun C, *et al.* (2024) Altered neurovascular coupling in patients with mitochondrial myopathy, encephalopathy, lactic acidosis, and stroke-like episodes (MELAS): a combined resting-state fMRI and arterial spin labeling study. *J Magn Reson Imaging* **60**:327–36.

Watts ME, Pocock R, Claudianos C (2018) Brain Energy and Oxygen Metabolism: Emerging Role in Normal Function and Disease. *Front Mol Neurosci* **11**:216.

Weinberger DR, Berman KF, Zec RF (1986) Physiologic dysfunction of dorsolateral prefrontal cortex in schizophrenia: I. Regional cerebral blood flow evidence. *Arch Gen Psychiatry* **43**:114–24.

Whitfield-Gabrieli S, Nieto-Castanon A (2012) Conn: a functional connectivity toolbox for correlated and anticorrelated brain networks. *Brain Connect* **2**:125–41.

Whitfield-Gabrieli S, Nieto-Castanon A, Ghosh S (2011) Artifact detection tools (ART), Neuroimaging Tools and Resources Collaboratory (NITRC), nitric.org.

Wu C, Wu H, Zhou C, *et al.* (2024) Neurovascular coupling alteration in drug-naïve Parkinson's disease: The underlying molecular mechanisms and levodopa's restoration effects. *Neurobiol Dis* **191**:106406.

Wu Y, Agarwal S, Jones CK, *et al.* (2016) Measurement of arteriolar blood volume in brain tumors using MRI without exogenous contrast agent administration at T7. *J Magn ResonImaging* **5**:1244–55.

Yan J, Chen Y, Ju P, *et al.* (2022)Network association of biochemical and inflammatory abnormalities with psychiatric symptoms in first-episode schizophrenia patients. *Front Psychiatry* **13**:834539.

Zhu J, Zhuo C, Qin W, *et al.* (2015) Altered resting-state cerebral blood flow and its connectivity in schizophrenia. *J Psychiatric Res* **63**:28–35.

Zhu J, Zhuo C, Xu L, *et al.* (2017) Altered coupling between resting-state cerebral blood flow and functional connectivity in schizophrenia. *Schizophr Bull* **43**:1363–74.

Zou QH, Zhu CZ, Yang Y, *et al.* (2008) An improved approach to detection of amplitude of low-frequency fluctuation (ALFF) for resting-state fMRI: fractional ALFF. *J Neurosci Methods* **172**:137–41.

**Received:** 7 November 2024; **Revised:** 31 December 2024; **Accepted:** 6 February 2025